Modeling derivative properties and binary mixtures with CO2 using the CPA and the quadrupolar CPA equations of state

Bjørner, Martin Gamel; Kontogeorgis, Georgios

Published in:
Fluid Phase Equilibria

Link to article, DOI:
10.1016/j.fluid.2016.04.019
10.1016/j.fluid.2015.08.011

Publication date:
2016

Document Version
Peer reviewed version

To further substantiate and facilitate the dissemination of results presented in the article "Modeling derivative properties and binary mixtures with CO_2 using the CPA and the quadrupolar CPA equations of state" some additional results are shown in this supporting materials. This concerns primarily results for derivative properties at saturation (both in the liquid and the gas phase) as well as additional visualizations of both pure and binary results. The nomenclature from the parent article is adopted.

1. Additional derivative property results

1.1. Saturation Region

Tables 1 and 2 compare the equations of state for their ability to predict several derivative properties at saturation in the liquid and vapor phase respectively ($T = 216 - 300$K). With the exception of $C_{P,liq}^{res,sat}$ it is observed that CPA n.a. often performs slightly better than the more sophisticated models. This is also the case for the heat of vaporization, where CPA n.a. seem to perform better, possibly due to a more accurate vapor phase enthalpy. Nevertheless, the difference is quite small and the performance of the various models is similar and mostly satisfactory.

Table 1: %AAD values of u_{liq}^{sat}, $C_{P,liq}^{res,sat}$, $C_{V,liq}^{res,sat}$, $\mu_{JT,liq}^{sat}$, and ΔH^{vap} for CO_2 at saturation using CPA n.a., CPA 4C and qCPA with three different parameter sets. The temperature range is $T = 216 - 300$K. Pseudo-experimental data from NIST [1]. u represents the speed of sound and μ_{JT} the Joule-Thomson coefficient.

Models	% AAD				
	u_{liq}^{sat}	$C_{P,liq}^{res,sat}$	$C_{V,liq}^{res,sat}$	$\mu_{JT,liq}^{sat}$	ΔH^{vap}
CPA, n.a.	13.2	7.6	10.7	6.6	7.7
CPA, 4C	13.2	4.8	35.1	8.7	9.9
qCPA, 3par	13.0	5.2	23.8	6.2	9.6
qCPA, 4par, set 1	13.0	5.1	27.5	7.6	10.6
qCPA, 4par, set 2	13.1	5.4	24.2	7.5	10

Figure 1 shows predictions of the liquid and vapor phase $C_P^{res,sat}$ (a) and $C_V^{res,sat}$ (b). It is clear from figure 1a that CPA 4C and qCPA predicts the liquid isobaric heat capacity very well as long as the critical point is not approached. On the other hand the trend of the liquid isochoric heat capacity is not captured by any of the models (figure 1b). In both cases the predictions in the vapor phase are quite poor.

Figure 2 illustrate that while the speed of sound in the vapor phase and the Joule-Thomson coefficient in the liquid phase are predicted quite well, the performance begins to deteriorate close to the critical point. The liquid phase speed of sound and vapor phase Joule-Thomson coefficient predictions are quantitatively wrong and moreover the trend of the data is not fully captured.

Table 2: % AAD values for ρ_{vap}^{sat}, u_{vap}^{sat}, $C_{P,vap}^{res,sat}$, $C_{V,vap}^{res,sat}$ and $\mu_{JT,vap}^{sat}$ at saturation using CPA n.a., CPA 4C and qCPA with three different parameter sets. The temperature range is $T = 216 - 300$K. Pseudo-experimental data from NIST [1].

Models	% AAD				
	ρ_{vap}^{sat}	u_{vap}^{sat}	$C_{P,vap}^{res,sat}$	$C_{V,vap}^{res,sat}$	$\mu_{JT,vap}^{sat}$
CPA, n.a.	6.9	6.2	56.7	86.4	9.1
CPA, 4C	8.1	5.7	57.1	79.1	10.5
qCPA, 3par	8.5	6.0	59.3	84.8	10.4
qCPA, 4par, set 1	9.5	6.0	60.6	84.5	11.0
qCPA, 4par, set 2	9.7	5.9	60.7	85.0	11.0

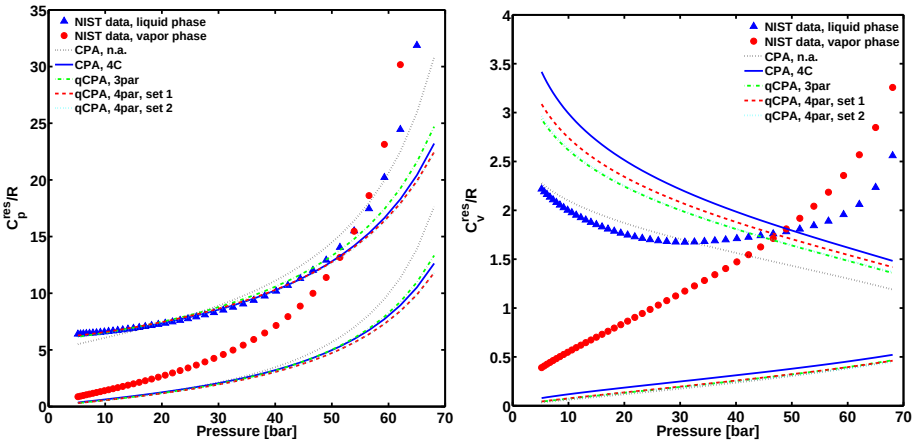

(a) (b)

Figure 1: Normalized liquid and vapor residual isochoric (a) and isobaric (b) heat capacity predictions of CO_2 at saturation with CPA and qCPA. Pseudo-experimental data from NIST [1].

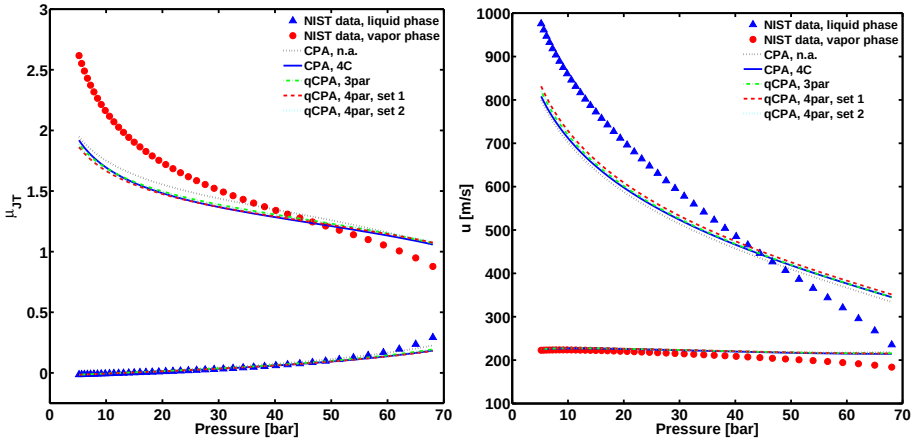

(a) (b)

Figure 2: Liquid and vapor Joule-Thomson coefficient (a) and speed of sound (b) predictions of CO_2 at saturation with CPA and qCPA. Pseudo-experimental data from NIST [1].

1.2. Compressed liquid region - Additional illustrations

Figure 3 shows that the speed of sound and Joule-Thomson prediction are slightly improved with qCPA and CPA 4C both of which suggest a slightly more accurate ratio between $(\partial P/\partial T)_{V,\mathbf{n}}$ and $(\partial P/\partial V)_{T,\mathbf{n}}$, even if part of the improvement in the speed of sound can be explained by a higher C_P/C_V ratio (see results in the article).

Using SAFT-VR Mie, Lafitte et al [2] found that the maximum in C_V could be predicted for 1-hexanol and 1-decanol. As the maximum was found to be mainly governed by the association term it is interesting that no such behaviour was observed when CO_2 was considered an associating compound. As the maximum in C_V for 1-hexanol is also predicted with CPA (see figure 4) we suspect, that the reason for the absence of this maximum for CO_2 is primarily due to the relatively small association parameters for CO_2.

Table 3 show the %AAD between model predictions and the density values from Brewer et al. [5].

Table 3: %AAD values between the experimental liquid density data of CO_2 from Brewer et al. [5] and the predicted values using cubic plus association (CPA) n.a., CPA 4C and quadrupolar CPA (qCPA) with three different parameter sets.

Model	T_r	CPA n.a.	CPA 4C	qCPA, 3par	qCPA, 4par, set1	qCPA, 4par, set 2
%AAD	0.9	1.4	1.2	1.1	1	1
%AAD	0.93	0.9	1.1	0.8	0.8	0.8

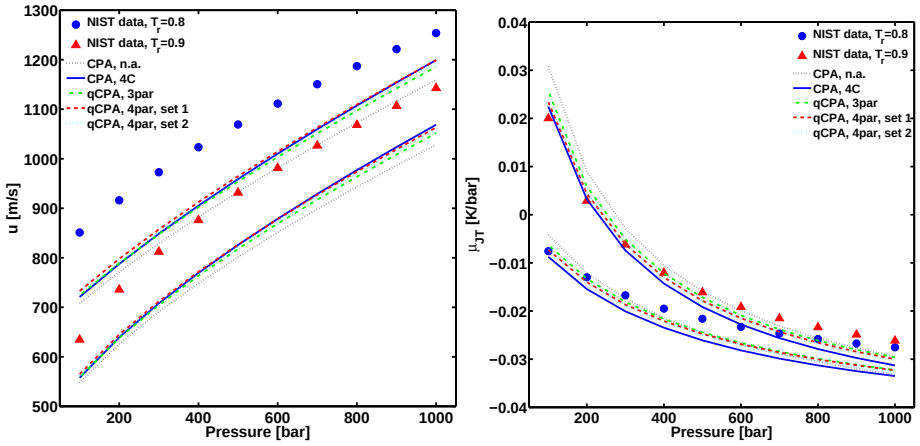

(a) (b)

Figure 3: Speed of sound (a) and Joule-Thomson coefficient (b) predictions of CO_2 with CPA and qCPA in the compressed liquid region and at $T_r = 0.8$ and 0.9. Pseudo-experimental data from NIST [1].

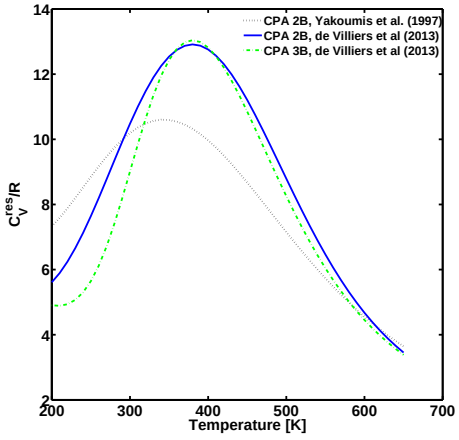

Figure 4: C_V^{res} predictions of 1-hexanol using 3 different CPA parameter sets with the 2B [3, 4] and 3B [4] schemes respectively. The parameters from de Villiers et al. [4] have been correlated to C_P^{liq} and ΔH^{vap} in addition to the saturated density and vapor pressure.

2. The CO_2 + propane VLE and CO_2 + n-dodecane LLE

The predicted CO_2 + propane VLE is shown in figure 5 at two temperatures. As parameter set 1 for qCPA has been selected partly based on the CO_2 + propane VLE it is not surprising that this parameter set results in the best predictions. Similarly parameter set 2 was selected partly based on the CO_2 + n-dodecane LLE. Figure 6 show that this parameter set yields excellent results for the LLE.

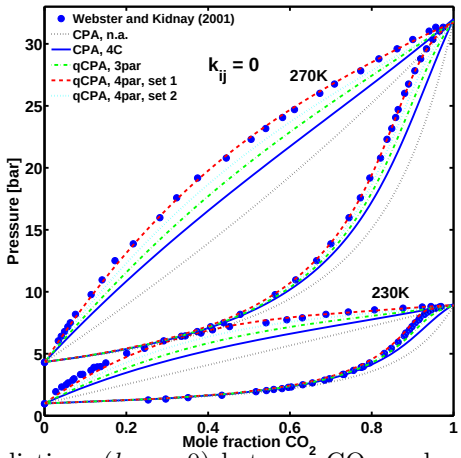

Figure 5: VLE predictions ($k_{ij} = 0$) between CO_2 and propane at 270K and 230K. Data from [6].

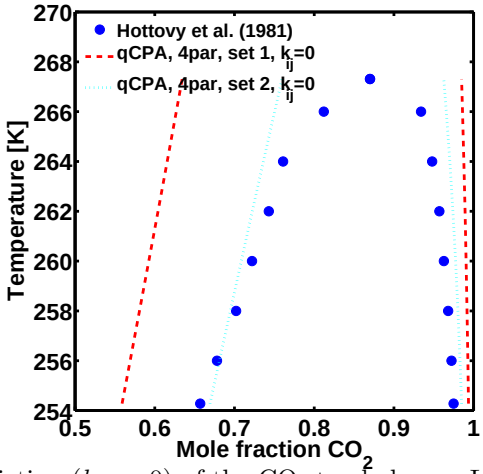

Figure 6: Prediction ($k_{ij} = 0$) of the CO_2+n-dodecane LLE. Data from [7].

References

[1] M. M. E.W. Lemmon, D. Friend, NIST Chemistry WebBook, NIST Standard Reference Database Number 69, National Institute of Standards and Technology, Gaithersburg MD, 20899, http://webbook.nist.gov, 2014, Ch. Thermophysical Properties of Fluid Systems.
URL http://webbook.nist.gov

[2] T. Lafitte, M. M. Piñeiro, J.-L. Daridon, D. Bessiéres, A comprehensive description of chemical association effects on second derivative properties of alcohols through a saft-vr approach, The Journal of Physical Chemistry B 111 (13) (2007) 3447–3461, pMID: 17388508. arXiv:http://dx.doi.org/10.1021/jp0682208, doi:10.1021/jp0682208.
URL http://dx.doi.org/10.1021/jp0682208

[3] I. V. Yakoumis, G. M. Kontogeorgis, E. C. Voutsas, D. P. Tassios, Vapor-liquid equilibria for alcoholhydrocarbon systems using the {CPA} equation of state, Fluid Phase Equilibria 130 (12) (1997) 31 – 47. doi:http://dx.doi.org/10.1016/S0378-3812(96)03200-1.
URL http://www.sciencedirect.com/science/article/pii/S0378381296032001

[4] A. de Villiers, C. Schwarz, A. Burger, G. Kontogeorgis, Evaluation of the pc-saft, {SAFT} and {CPA} equations of state in predicting derivative properties of selected non-polar and hydrogen-bonding compounds, Fluid Phase Equilibria 338 (0) (2013) 1 – 15. doi:http://dx.doi.org/10.1016/j.fluid.2012.09.035.
URL http://www.sciencedirect.com/science/article/pii/S0378381212004839

[5] P. G. Brewer, G. Friederich, E. T. Peltzer, F. M. Orr, Direct experiments on the ocean disposal of fossil fuel co2, Science 284 (5416) (1999) 943–945. arXiv:http://www.sciencemag.org/content/284/5416/943.full.pdf, doi:10.1126/science.284.5416.943.
URL http://www.sciencemag.org/content/284/5416/943.abstract

[6] L. A. Webster, A. J. Kidnay, Vapor-liquid equilibria for the methan-propane-carbon dioxide systems at 230 k and 270 k, Journal of Chemical & Engineering Data 46 (3) (2001) 759–764. arXiv:http://dx.doi.org/10.1021/je000307d, doi:10.1021/je000307d.
URL http://dx.doi.org/10.1021/je000307d

[7] J. D. Hottovy, K. D. Luks, J. P. Kohn, Three-phase liquid-liquid-vapor equilibriums behavior of certain binary carbon dioxide-n-paraffin systems, Journal of Chemical & Engineering Data 26 (3) (1981) 256–258. arXiv:http://dx.doi.org/10.1021/je00025a009, doi:10.1021/je00025a009.
URL http://dx.doi.org/10.1021/je00025a009